

## NH<sub>3</sub>-induced removal of NO<sub>x</sub> from a flue gas stream by silent discharge ozone generation in a double reactor system

Yujin Hwang<sup>\*,‡</sup>, Abid Farooq<sup>\*,‡</sup>, Sung Hoon Park<sup>\*\*,‡</sup>, Ki Hoon Kim<sup>\*</sup>, Myong-Hwa Lee<sup>\*\*\*</sup>,  
Seuk Cheun Choi<sup>\*\*\*\*</sup>, Min Young Kim<sup>\*\*</sup>, Rae-su Park<sup>\*\*\*\*\*</sup>, and Young-Kwon Park<sup>\*,†</sup>

<sup>\*</sup>School of Environmental Engineering, University of Seoul, Seoul 02504, Korea

<sup>\*\*</sup>Department of Environmental Engineering, Sunchon National University, Suncheon 57922, Korea

<sup>\*\*\*</sup>Department of Environmental Engineering, Kangwon National University, Chuncheon 24341, Korea

<sup>\*\*\*\*</sup>Thermochemical Energy System R&D Group, Korea Institute of Industrial Technology, Cheonan 31056, Korea

<sup>\*\*\*\*\*</sup>Department of Bioenvironmental & Chemical Engineering, Chosun College of Science & Technology, Gwangju 501-744, Korea

(Received 11 April 2019 • accepted 12 June 2019)

**Abstract**—NO<sub>x</sub>, a generic term for the nitrogen oxides generated from combustion in the presence of nitrogen, is a serious threat to human health. This study examined the removal of NO<sub>x</sub> using ammonia (NH<sub>3</sub>) and ozone produced using a silent discharge method. The effects of temperature and residence time on NO<sub>x</sub> removal with NH<sub>3</sub> injection in a double reactor system were investigated. An increase in temperature resulted in higher levels of O<sub>3</sub> decomposition, whereas the maximum particle formation in the form of ammonium nitrate (NH<sub>4</sub>NO<sub>3</sub>) was achieved when both reactors were kept at 180 °C. NH<sub>3</sub> and O<sub>3</sub> injection in large quantities and NO in smaller amounts with a residence time of 10.2 s resulted in the maximum particulate formation. In contrast, when an excess of NH<sub>3</sub> was supplied, it resulted in N<sub>2</sub>O formation due to the formation of NH<sub>2</sub> radicals generated from a reaction of NO<sub>2</sub> with NH<sub>3</sub>. In addition, 100% NO removal was achieved regardless of the residence time. Kinetic simulations indicated the possibility of moisture being the limiting reactant.

Keywords: Ozone, NO<sub>x</sub> Removal, Flue Gas, Ammonium Nitrate, Ammonia

### INTRODUCTION

With the increasing demand for, and consumption of, fossil fuels, nitrogen oxides (NO<sub>x</sub>) from stationary flue gas emissions pose a serious threat to human health, the ecosystem and the atmosphere [1,2]. Approximately 90% of the total NO<sub>x</sub> emission from stationary sources is from vehicle exhaust and other stationary combustion sources (industries) [3]. NO<sub>x</sub> is the major pollutant responsible for the generation of acid rain/acid mist and triggers photochemical reactions when combined with hydrocarbons, resulting in the generation of haze and smog. Therefore, it is important to develop NO<sub>x</sub> removal technology to remediate environmental pollution.

Several NO<sub>x</sub> emission control technologies have been developed to counter this problem, including NO<sub>x</sub> storage reduction systems for lean burn engines [4], selective catalytic reduction (SCR) for large scale combustion facilities [5], and three-way catalysts for gasoline fueled vehicles [6]. Among all the NO<sub>x</sub> reduction technologies, the conversion of NO to N<sub>2</sub> and O<sub>2</sub> appears to be the most desirable process, but the high temperature requirements and presence of O<sub>2</sub> inhibiting conversion are major difficulties [7]. Pulsed corona or E-beam has attracted recent attention as a denitrification process.

Non-thermal plasma is regarded as one of the most viable processes among the potential technologies [8].

Several studies have examined the non-thermal plasma process for denitrification (removal of NO<sub>x</sub>) from flue gases and stationary combustion sources, such as diesel power generators, incinerators, and boilers [9-12]. Tsukamoto et al. [13] examined NO<sub>x</sub> and SO<sub>2</sub> removal at a thermal power plant using pulsed power (non-thermal plasma) and reported that 90% of NO and SO<sub>2</sub> was removed from the flue gases at the repetition rate of seven pulses/sec and a flow rate of 0.8 l/min. Lin et al. [14] examined NO<sub>x</sub> removal by plasma-assisted radical injection and NaOH scrubbing. The results revealed a de-NO<sub>x</sub> efficiency of 81.2%. Mizuno et al. [15] examined the NO<sub>x</sub> removal process using non equilibrium pulse discharged plasma in a simulated flue gas. NO<sub>x</sub> reduction from 800 ppm to 300 ppm was observed as a result. Chae [16] reported the mechanism of the use of non-thermal plasma for the treatment of flue gases coming out of diesel exhaust. He deduced that the use of non-thermal induced plasma is a key process for the oxidation of NO to NO<sub>2</sub> and the catalyst system with plasma can achieve high conversion at low temperatures. Furthermore, high particulate removal was observed in the case of plasma.

Many studies have applied hybrid technology to remove NO<sub>x</sub> from flue gas streams [17-21]. Yamamoto et al. [17] investigated the removal of NO<sub>x</sub> and SO<sub>x</sub> simultaneously from flue gas coming out of a glass melting furnace by a semi-dry chemical process and ozone injection combined. They observed the effective oxidation

<sup>†</sup>To whom correspondence should be addressed.

E-mail: catalica@uos.ac.kr

<sup>‡</sup>Co-first authors

Copyright by The Korean Institute of Chemical Engineers.

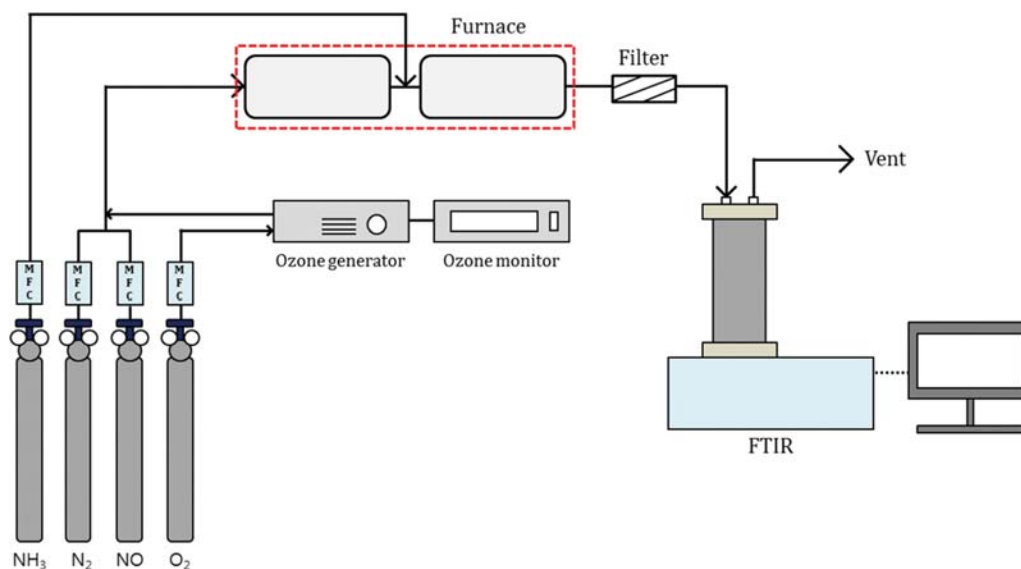


Fig. 1. Schematics of experimental setup.

of NO to NO<sub>2</sub> with the injection of O<sub>3</sub> in the spray region, whereas the removal efficiency of NO and NO<sub>2</sub> was 90% and 50%, respectively. In addition, they achieved 84% removal efficiency for SO<sub>2</sub>. Onda et al. [20] performed numerical analysis on the removal of NO<sub>x</sub> using an ammonia-assisted pulsed-discharge. They determined that the removal efficiencies for NO increase with increasing electric energy consumption rate in the case of ammonia injection. In contrast, the NO<sub>x</sub> removal efficiency declined when excess ammonia was supplied because of the formation of N<sub>2</sub>O, a relatively stable compound. Cha et al. [22] examined NO<sub>x</sub> removal from 300 hp marine diesel engine exhaust by combining two techniques: selective catalytic reduction using ammonia and the removal of NO<sub>x</sub> using non-thermal plasma in a low temperature range of 100–200 °C. They observed a four-fold increase from 20% to 80% in the de-NO<sub>x</sub> efficiency at 100 °C compared to SCR alone. In addition, a more than 45% decrease in particulate matter (PM) and a significant alteration in the size distribution of PM after the plasma process were detected.

This study investigated the effects of ammonia injection with respect to temperature and residence time on the removal of NO<sub>x</sub> using silent discharge ozone generation in a double reactor system from a flue gas stream. Two reactors were placed in a series where the NO and O<sub>3</sub> reaction was carried out in the first reactor, and the second reactor was for NO<sub>2</sub> conversion to a solid form. Ammonia was injected between the two reactors to achieve the maximum conversion of NO<sub>x</sub>. The effects of temperature and residence time on NO conversion were investigated. FTIR spectroscopy was performed to analyze the products after the completion of the reaction. Moreover, the effects of these parameters on particle formation were discussed.

## EXPERIMENTAL

The materials used for the process were N<sub>2</sub>, O<sub>2</sub>, NO, and NH<sub>3</sub> contained in cylinders, whereas ozone (O<sub>3</sub>) was generated by an ozone generator and the quantity produced was monitored using an

ozone monitor. Fig. 1 presents a schematic diagram of the experimental setup which consisted of four cylinders containing NH<sub>3</sub>, N<sub>2</sub>, NO, and O<sub>2</sub> along with an ozone generator (OWONE TECH, Ozone generator, LAB-II) and an ozone monitor. The ozone was generated using a silent discharge method. The cylinders were connected to the reactors with stainless steel connecting the lines. The system consisted of two cylindrical reactors, with 30 cm in length and 6 cm in diameter. The ammonia line was connected between the two reactors. The flow rates of all the gases were controlled using mass flow meters. The reactors were followed by a filter and Fourier transform infrared refractometer (FTIR) to observe the functional groups in the product gas. Overall, the system is very sophisticated for the removal of NO<sub>x</sub> from a flue gas stream on the laboratory scale.

As for the methodology, both the reactors were purged with nitrogen for 60 minutes before the start of experiment. After purging, the temperature of the reactors was raised to the required value. The temperature was measured with a thermocouple attached to each reactor. After reaching the required temperature, the O<sub>3</sub> was generated in the ozone generator (OWONE TECH, Ozone generator, LAB-II) using a silent discharge method and was injected along with other feed gases (NO and N<sub>2</sub>) into the first reactor, whereas NH<sub>3</sub> was injected into the second reactor. The residence time was controlled by the change in the flow rate of nitrogen, and the reaction was allowed to continue for 6 hr for the generation of solid particles. During the reaction, the product gases were allowed to pass directly to the FTIR attached to the outlet for functional group analysis. The reactors were purged again for 60 min after the completion of reaction to decrease the temperature inside the reactor, and both the reactors were dis-assembled for the collection of solid particles and weight measurement.

## REACTION MECHANISM AND KINETIC SIMULATIONS

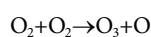
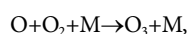
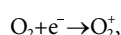
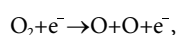
The ozone generation can be explained by the following mech-

**Table 1. Reaction rate constants of the reactions considered**

Reaction number	Reaction equation	Reaction rate constant (cm <sup>3</sup> /molecules/s*)	Reaction rate constant at 180 °C
Furnace 01			
R05	NO+O <sub>3</sub> →NO <sub>2</sub> +O <sub>2</sub>	1.4E-12exp(-1310/T)	7.774×10 <sup>-14</sup>
R06	NO <sub>2</sub> +O <sub>3</sub> →NO <sub>3</sub> +O <sub>2</sub>	1.4E-13exp(-2470/T)	6.010×10 <sup>-16</sup>
R07	NO <sub>3</sub> →NO+O <sub>2</sub>	-	-
R08	NO <sub>2</sub> +NO <sub>3</sub> →N <sub>2</sub> O <sub>5</sub>	k <sub>0</sub> =3.6E-30(T/300) <sup>-4.1</sup> [N <sub>2</sub> ] k <sub>c</sub> =1.9E-12(T/300) <sup>0.2</sup> F <sub>C</sub> =0.35	4.244×10 <sup>-13</sup>
R09	2NO <sub>2</sub> +H <sub>2</sub> O→HNO <sub>2</sub> +HNO <sub>3</sub>	3.61×10 <sup>-17</sup> T <sup>-1.489</sup> exp(-2121/T)	3.019×10 <sup>-15</sup>
R10	H <sub>2</sub> O+N <sub>2</sub> O <sub>5</sub> →2HNO <sub>3</sub>	9.51×10 <sup>-17</sup> (T/298 K) <sup>3.354</sup> exp(-7900 K/T)	1.041×10 <sup>-23</sup>
R11	2HNO <sub>2</sub> →NO+NO <sub>2</sub> +H <sub>2</sub> O	1.32×10 <sup>-24</sup> T <sup>3.36</sup> exp(-6764/T)	3.656×10 <sup>-22</sup>
Furnace 02			
R13	HNO <sub>3</sub> +NH <sub>3</sub> →NH <sub>4</sub> NO <sub>3</sub>	1.05E-7	1.050×10 <sup>-7</sup>
R14	NH <sub>4</sub> NO <sub>3</sub> →N <sub>2</sub> O+2H <sub>2</sub> O	8.1×10 <sup>16</sup> T <sup>-1.44</sup> exp(-135/T)	-

\*Except R9 whose rate constant has the unit of cm<sup>6</sup>/molecules<sup>2</sup>/s

anism [23]:



The reaction mechanism for determining the kinetics of the process can be explained using the following reactions [9,24,25]



NH<sub>4</sub>NO<sub>3</sub> is formed as a result of a reaction between NH<sub>3</sub> with HNO<sub>3</sub> [26].



The decomposition of NH<sub>4</sub>NO<sub>3</sub> results in the formation of N<sub>2</sub>O and H<sub>2</sub>O [27],



When a suitable amount of NH<sub>3</sub> is available, the removal of NO<sub>2</sub> is achieved with the formation of solid NH<sub>4</sub>NO<sub>3</sub>. In contrast, if ammonia is supplied in an excess of NO<sub>2</sub>, N<sub>2</sub>O [20,25], a greenhouse gas, is formed with the release of a large amount of NH<sub>2</sub> as a result of the pulse discharge.



Kinetic simulations were carried out based on the above-mentioned reaction mechanism to interpret the experimental results. The reaction mechanism given here is a stiff system because many reactions need to be considered and the reaction rates are quite diverse. Therefore, the reactions, whose reaction rates are relatively high, were selected. In addition, the reactions involving electron, oxygen atom, and OH radical were excluded because their concentrations could not be measured. Table 1 lists the reactions and corresponding reaction rate constants available in the literature.

Table 1 shows that R09 and R13 would have much higher reaction rates than other reactions. Therefore, it is expected that the formation of NH<sub>4</sub>NO<sub>3</sub> is led mostly by R05, R09, and R13. Furnace 01 was simulated using R05 and R09, whereas Furnace 02 was simulated using R13 only. The fifth-order Runge-Kutta method was used for numerical integration.

## RESULTS AND DISCUSSION

### 1. Effects of Temperature

Fig. 2 shows the effect of the reactor temperature on O<sub>3</sub> decomposition and corresponding FTIR spectra. An increasing trend in O<sub>3</sub> decomposition (Fig. 2(a)) was observed with increasing temperature. The effect has been translated to FTIR spectra, as shown in Fig. 2(b); the lowest peak in terms of absorbance corresponds to the highest temperature (200 °C), whereas the highest can be seen corresponding to the lowest temperature (120 °C).

Fig. 3 presents the effects of temperature on particle formation, while Fig. 4 shows the effects of temperature on O<sub>3</sub> and NH<sub>3</sub> consumption. Three combinations (180 °C-150 °C, 180 °C-180 °C, and

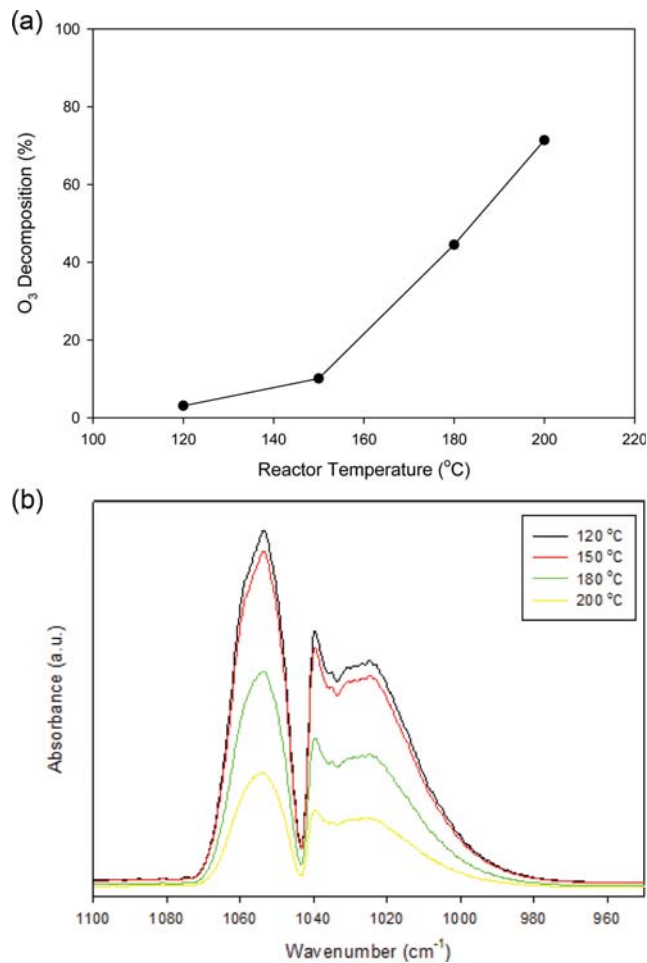


Fig. 2. (a) Effect of Temperature on O<sub>3</sub> decomposition, (b) FTIR at different temperatures.

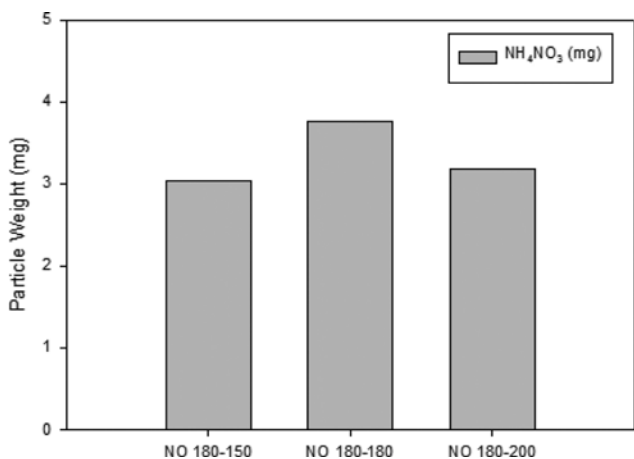


Fig. 3. Effect of temperature on NH<sub>4</sub>NO<sub>3</sub> formation.

180 °C-200 °C) for the temperatures of the first and second reactors were investigated to determine the optimal particle formation conditions with an NO and NH<sub>3</sub> concentration of 35 ppm and 66 ppm, respectively. The maximum particle formation was observed when the temperature for both reactors was kept at 180 °C. There-

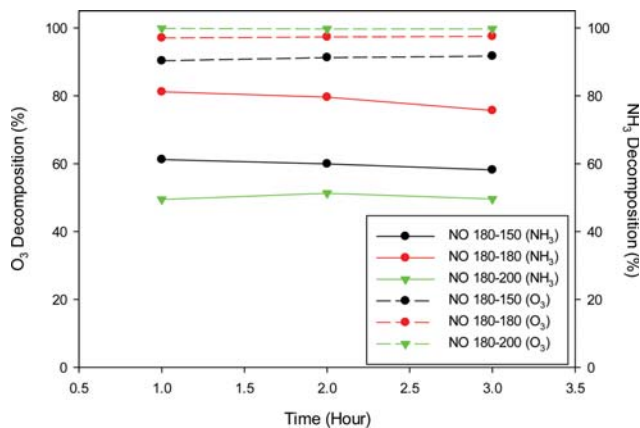


Fig. 4. O<sub>3</sub> and NH<sub>3</sub> consumption rates at different times.

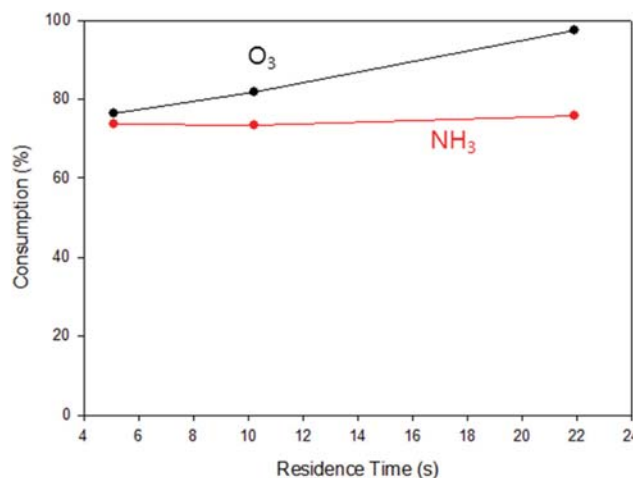


Fig. 5. Effect of residence time on consumption of O<sub>3</sub> and NH<sub>3</sub>.

fore, 180 °C was considered the optimal temperature because it gives the maximum consumption of NH<sub>3</sub> and optimal O<sub>3</sub> decomposition for the maximum NO removal and NH<sub>4</sub>NO<sub>3</sub> formation, as shown in Fig. 3 and Fig. 4. Higher conversion to NH<sub>4</sub>NO<sub>3</sub> corresponds to the higher consumption of O<sub>3</sub> for NO to NO<sub>2</sub> conversion and then NO<sub>2</sub> to NH<sub>4</sub>NO<sub>3</sub> with a higher consumption of ammonia. The process can be further explained by the following reaction [20]:



The NO in the above equation is neutralized with the injection of ammonia, resulting in the conversion of NH<sub>4</sub>NO<sub>3</sub>. On the other hand, a part of NO<sub>x</sub> was also removed and reduced by NH<sub>2</sub> and N radicals formed by NH<sub>3</sub>.

### 2. Effect of Residence Time

Fig. 5 shows the effects of residence time on O<sub>3</sub>, NH<sub>3</sub> consumption. The maximum consumption of O<sub>3</sub> and NH<sub>3</sub> was observed at a residence time of 21.9 s and 10.2 s, respectively. Moreover, O<sub>3</sub> consumption increased with increasing residence time but NH<sub>3</sub> remained relatively constant after 10.2 s. Therefore, 10.2 s was considered to be the optimal point in terms of ammonia consumption for the conversion of NO to NO<sub>2</sub>. Moreover, the optimal point in terms

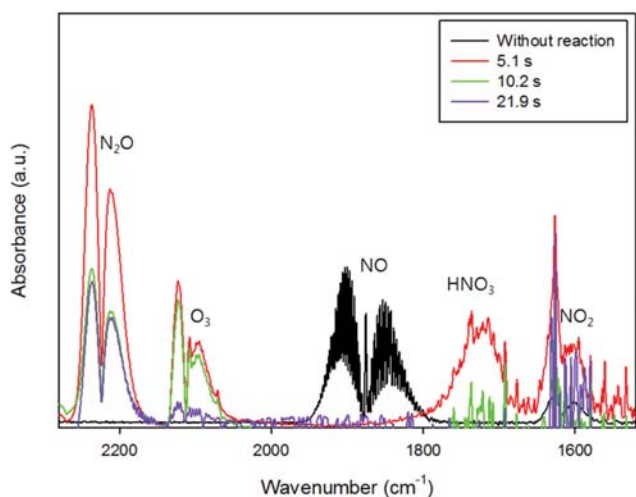


Fig. 6. Effect of residence time on chemical species distribution.

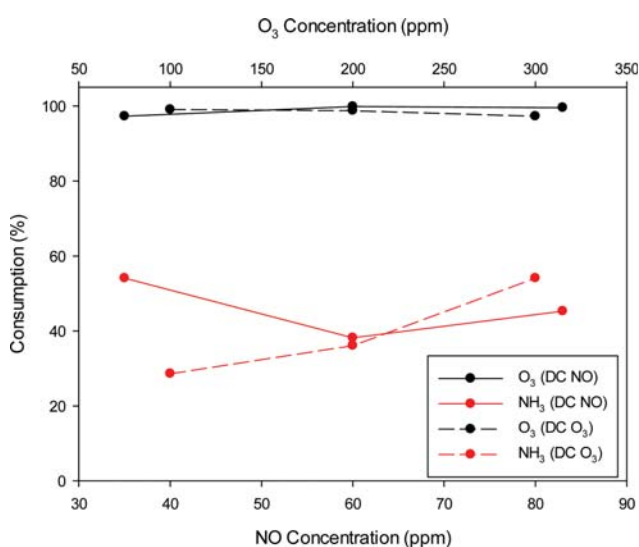


Fig. 7. Effect of injected O<sub>3</sub> and NO concentrations on gas consumption in 10.2 s (DC NO: different concentration of NO, DC O<sub>3</sub>: different concentration of O<sub>3</sub>).

of residence time could only be decided after particle generation, discussed later in this section. In contrast, NO removal remained at 100%, irrespective of the residence time, as shown in Fig. S1. O<sub>3</sub> and NH<sub>3</sub> consumption is the major factor involved in the conversion of NO<sub>x</sub> explained in the next sections.

The IR peaks in Fig. 6 show the effects of residence time on NO consumption and NO<sub>x</sub> generation. The peaks represent 100% NO removal, irrespective of the residence time. In contrast, the highest peaks for N<sub>2</sub>O and NO<sub>2</sub> were observed at a residence time of 5.1 s. The effect corresponds to the excess of NH<sub>3</sub> [20] in the reactor and insufficient time for the reaction to be completed explained in Eq. (15)-(18). On the other hand, the generation of N<sub>2</sub>O and NO<sub>2</sub> was reduced along with less HNO<sub>3</sub> generation, suggesting more production of solid particles in the system. The residence time of 21.9 s resulted in more NO<sub>2</sub> generation with more N<sub>2</sub> injection.

The O<sub>3</sub> concentration plays a vital role in the generation of NO<sub>x</sub>.

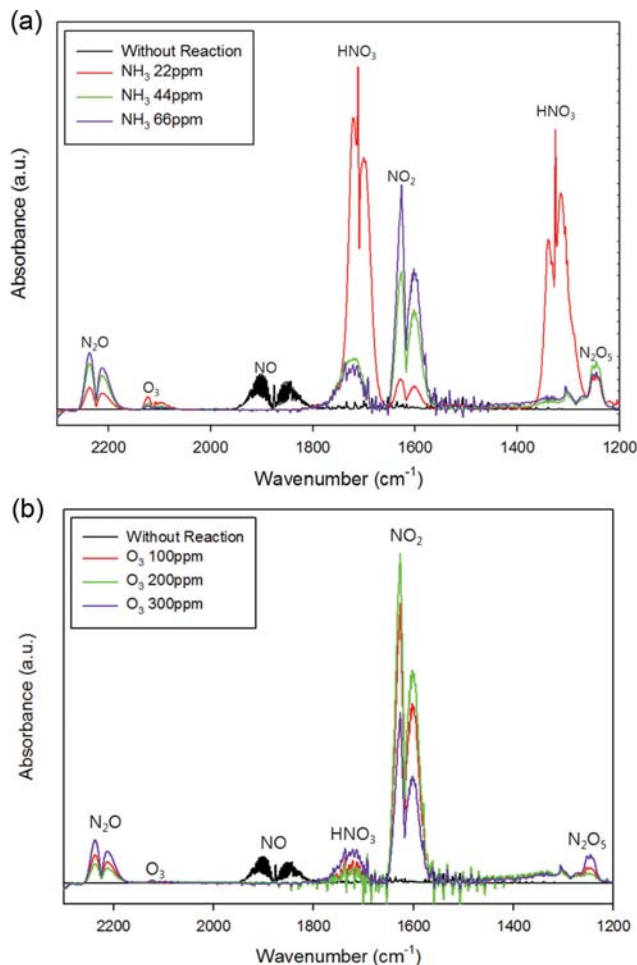


Fig. 8. Effect of injected (a) NH<sub>3</sub> and (b) O<sub>3</sub> concentrations in 10.2 s.

Fig. 7 presents the effects of the O<sub>3</sub> and NO concentration on gas consumption. The maximum NH<sub>3</sub> consumption was observed at 300 ppm of O<sub>3</sub> injection; hence, this was considered to be the optimal O<sub>3</sub> concentration for the process as more NH<sub>3</sub> consumption corresponds to more NH<sub>4</sub>NO<sub>3</sub> generation, as explained in Eq. (19). On the other hand, the excess ammonia can result in more N<sub>2</sub>O generation due to the formation of a NH<sub>2</sub> radical produced as a result of electron collision [20] when NH<sub>3</sub> reacts with NO<sub>2</sub>, as shown in Eqs. (15) and (16). Therefore, it is imperative to perform a stoichiometric calculation before the start of the experiment to inject the required amount of gases. The effect can be observed in Fig. 8(a) and 8(b). The maximum N<sub>2</sub>O generation can be seen when 66 ppm and 300 ppm of NH<sub>3</sub> and ozone, respectively, were supplied. Moreover, more NH<sub>3</sub> and O<sub>3</sub> consumption resulted in more particle formation, which is easy to collect, whereas more generation of HNO<sub>3</sub> was observed at low NH<sub>3</sub> concentrations. High NH<sub>3</sub> consumption was observed in the case of 35 ppm of NO, whereas very little change in O<sub>3</sub> consumption was noted throughout the process. Therefore, 35 ppm of NO can be considered the optimal amount to be provided in the process for maximum particle formation (Fig. S2). The lower peaks of NO<sub>2</sub> can be seen with 35 ppm of NO and a higher peak trend was observed with increasing NO concentration.

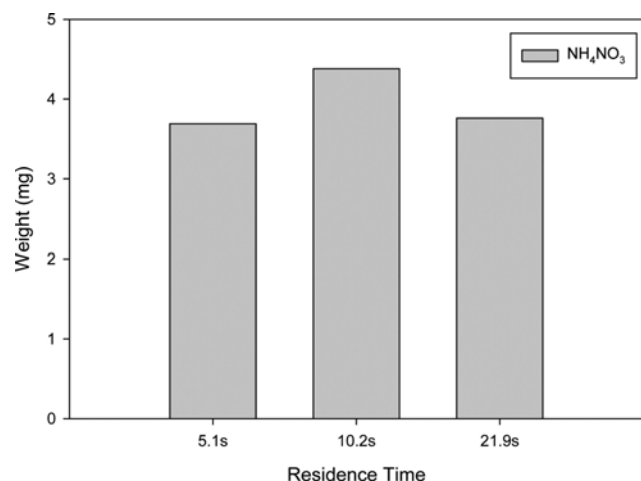


Fig. 9. Effect of residence time on particle formation.

Fig. 9 shows the effects of residence time on particle ( $\text{NH}_4\text{NO}_3$ ) formation. The maximum amount of particle formation (4.38 mg) was observed with a residence time of 10.2 s. The effects were due to the larger amount of  $\text{NH}_3$  (66 ppm) and  $\text{O}_3$  (300 ppm) injection and the lower amount of NO (35 ppm) at the injection point of the second reactor. The higher particle formation was attributed to the  $\text{NH}_3$  injection, resulting in the reaction between  $\text{NH}_3$  and  $\text{HNO}_3$  promoting the oxidation removal process, as shown in Eq. (19). The  $\text{NH}_3$ ,  $\text{O}_3$ , and NO concentration was chosen based on the IR peaks. The selected concentrations result in the generation of less  $\text{NO}_x$  and more solid particles ( $\text{NH}_4\text{NO}_3$ ), which can be removed easily from the reactor.

### 3. Kinetic Simulations

Initially, the model was run with excess moisture because there is no information on the moisture content. R05 and R09 ended very quickly ( $t < 0.01$  s) owing to the depletion of  $\text{O}_3$ . The amount of  $\text{HNO}_3$  produced was half that of  $\text{O}_3$  introduced to the reactor, which is consistent with the stoichiometry of R05 and R09. The amount of  $\text{NH}_4\text{NO}_3$  produced in Furnace 02 was the same as that of  $\text{HNO}_3$  introduced into the furnace.

On the other hand, the amount of  $\text{NH}_4\text{NO}_3$  collected from Furnace 02 during the experiments was a factor of 10,000 smaller than the model prediction. This suggests that the furnace may have been under oxygen-poor conditions. Therefore, the supply of moisture into the reactor may be a way to promote the conversion of NO to  $\text{NH}_4\text{NO}_3$ . More study will be needed to examine the effects of moisture in the future. Another issue is the effects of oxidizing radicals, such as O and OH, which could not be quantified in this study because of the lack of measurement. This should be another topic of future study.

### CONCLUSION

The  $\text{NH}_3$ -induced removal of  $\text{NO}_x$  using silent discharge ozone generation with respect to temperature and residence time in a double reactor system was investigated and the following conclusions were made:

- Ozone ( $\text{O}_3$ ) decomposition increased with increasing tem-

perature, while maximum particle formation was obtained with the temperature combination of 180 °C-180 °C. The effect was attributed to the maximum consumption of ammonia in this temperature range.

- The consumption of  $\text{O}_3$  increased with increasing residence time, whereas the consumption of  $\text{NH}_3$  was relatively constant with increasing residence time.

- NO removal was 100%, irrespective of the residence time.

- The residence time of 10.2 s,  $\text{NH}_3$  injection of 66 ppm,  $\text{O}_3$  injection of 100 ppm, and NO injection of 35 ppm resulted in the maximum particle formation, which is easy to collect and safer for the environment.

- Ammonium nitrate ( $\text{NH}_4\text{NO}_3$ ) was formed after  $\text{NH}_3$  injection due to the reaction between  $\text{NH}_3$  and  $\text{HNO}_3$ , promoting the oxidation removal process. The process was also promoted by the formation of  $\text{NH}_2$  radicals formed due to the electron collision dissociation of  $\text{NH}_3$ . Both processes improved the  $\text{NO}_x$  removal performance.

- The formation of  $\text{N}_2\text{O}$  occurred as a result of a  $\text{NH}_2$  radical reaction with  $\text{NO}_2$  formed due to electron collision with ammonia when an excess of  $\text{NH}_3$  and shorter residence time was supplied.

- Kinetic simulations indicated that moisture might have been the limiting reactant for the formation of  $\text{NH}_4\text{NO}_3$ . More study will be needed to quantify the effects of moisture and oxidizing radicals.

### ACKNOWLEDGEMENTS

This research was supported by the National Strategic Project-Fine particle of the National Research Foundation of Korea (NRF) funded by the Ministry of Science and ICT (MSIT), the Ministry of Environment (ME), and the Ministry of Health and Welfare (MOHW) (2017M3D8A1092029).

### SUPPORTING INFORMATION

Additional information as noted in the text. This information is available via the Internet at <http://www.springer.com/chemistry/journal/11814>.

### REFERENCES

1. Y. Xiong, Y. Zeng, W. Cai, S. Zhang, J. Ding and Q. Zhong, *J. Ind. Eng. Chem.*, **65**, 380 (2018).
2. X. Long, B. Duan, H. Cao, M. Jia and L. Wu, *J. Ind. Eng. Chem.*, **62**, 217 (2018).
3. H. Wang, X. Li, P. Chen, M. Chen and X. Zheng, *Chem. Commun.*, **49**, 9353 (2013).
4. S. Roy and A. Baiker, *Chem. Rev.*, **109**, 4054 (2009).
5. Y. Fan, W. Ling, B. Huang, L. Dong, C. Yu and H. Xi, *J. Ind. Eng. Chem.*, **56**, 108 (2017).
6. M. Shelef and R. W. McCabe, *Catal. Today*, **62**, 35 (2000).
7. F. Garin, *Appl. Catal. A: Gen.*, **222**, 183 (2001).
8. S. Tsukamoto and T. Namihira, Pulsed Power Conference, Monterey, CA, 1330 (1999).
9. J. O. Chae, *J. Electrostatics*, **57**, 251 (2003).
10. J. O. Jo and Y. S. Mok, *Appl. Chem. Eng.*, **29**, 92 (2018).

11. H. Fujishima, K. Takekoshi, T. Kuroki, A. Tanaka, K. Otsuka and M. Okubo, *Appl. Energy*, **111**, 394 (2013).
12. T. Kuroki, M. Takahashi, M. Okubo and T. Yamamoto, *IEEE Trans. Ind. Appl.*, **38**, 1204 (2002).
13. S. Tsukamoto, T. Namihira, D. Wang, S. Katsuki, H. Akiyama and E. Nakashima, Digest of Technical Papers 12<sup>th</sup> IEEE International Pulsed Power Conference (Cat No99CH36358), 2, 1330 (1999).
14. H. Lin, X. Gao, Z. Y. Luo, S. P. Guan, K. F. Cen and Z. Huang, *J. Environ. Sci. (China)*, **16**, 462 (2004).
15. A. Mizuno, R. Shimizu, A. Chakrabarti, L. Dascalescu and S. Furuta, *IEEE Trans. Ind. Appl.*, **31**, 957 (1995).
16. J. O. Chae, *J. Electrostatics*, **57**, 251 (2003).
17. Y. Yamamoto, H. Yamamoto, D. Takada, T. Kuroki, H. Fujishima and M. Okubo, *Ozone: Sci. Eng.*, **38**, 211 (2016).
18. H. W. Park and S. Uhm, *Appl. Chem. Eng.*, **28**, 607 (2017).
19. J. S. Cha, J. W. Park, B. Jeong, H. D. Kim, S. S. Park and M. C. Shin, *Appl. Chem. Eng.*, **28**, 576 (2017).
20. O. Kazuo, K. Hironobu, I. Kohei and H. Ibaraki, *J. Appl. Phys.*, **95**, 3928 (2004).
21. B. Guan, H. Lin, Q. Cheng and Z. Huang, *Ind. Eng. Chem. Res.*, **50**, 5401 (2011).
22. M. S. Cha, Y.-H. Song, J.-O. Lee and S. J. Kim, *Int. J. Plasma Environ. Sci. Technol.*, **1**, 28 (2007).
23. J. Kitayama and M. Kuzumoto, *J. Phys. D: Appl. Phys.*, **30**, 2453 (1997).
24. K. Nishimura and N. Suzuki, *J. Nuclear Sci. Technol.*, **18**, 878 (1981).
25. R. Atkinson, D. L. Baulch, R. A. Cox, J. N. Crowley, R. F. Hampson and R. G. Hynes, *Atmos. Chem. Phys.*, **4**, 1461 (2004).
26. D.-J. Kim, Y. Choi and K.-S. Kim, *Plasma Chem. Plasma Process.*, **21**, 625 (2001).
27. G. Feick and R. M. Hainer, *J. Am. Chem. Soc.*, **76**, 5860 (1954).

## Supporting Information

### **NH<sub>3</sub>-induced Removal of NO<sub>x</sub> from a flue gas stream by silent discharge ozone generation in a double reactor system**

Yujin Hwang<sup>\*,‡</sup>, Abid Farooq<sup>\*,‡</sup>, Sung Hoon Park<sup>\*\*,‡</sup>, Ki Hoon Kim<sup>\*</sup>, Myong-Hwa Lee<sup>\*\*\*</sup>,  
Seuk Cheun Choi<sup>\*\*\*\*</sup>, Min Young Kim<sup>\*\*</sup>, Rae-su Park<sup>\*\*\*\*\*</sup>, and Young-Kwon Park<sup>\*,†</sup>

<sup>\*</sup>School of Environmental Engineering, University of Seoul, Seoul 02504, Korea

<sup>\*\*</sup>Department of Environmental Engineering, Sunchon National University, Suncheon 57922, Korea

<sup>\*\*\*</sup>Department of Environmental Engineering, Kangwon National University, Chuncheon 24341, Korea

<sup>\*\*\*\*</sup>Thermochemical Energy System R&D Group, Korea Institute of Industrial Technology, Cheonan 31056, Korea

<sup>\*\*\*\*\*</sup>Department of Bioenvironmental & Chemical Engineering, Chosun College of Science & Technology,  
Gwangju 501-744, Korea

(Received 11 April 2019 • accepted 12 June 2019)

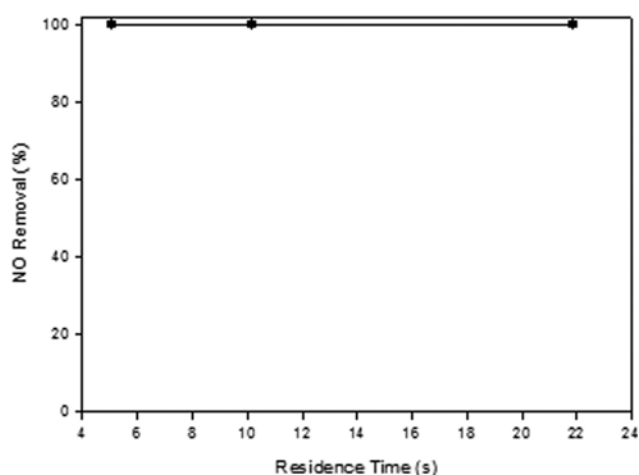


Fig. S1. Effect of residence time on NO removal.

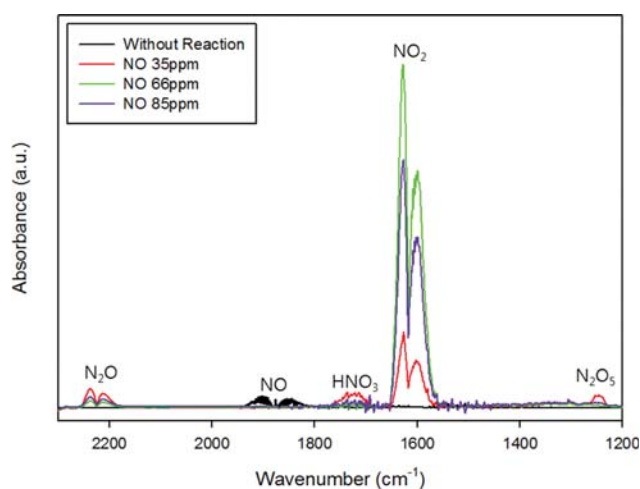


Fig. S2. Effect of injected NO concentration on NO removal in 10.2 s.